# The utilities of U-shape EM sensor in stress monitoring

Guodun Wang† and Ming L. Wang‡

*Department of Civil and Materials Engineering, The University of Illinois at Chicago, Chicago,
IL 60607, U.S.A.*

**Abstract.** In this paper, load monitoring technologies using U-shape Magnetoelastic (EM or ME) sensors have been exploited systemically for the first time. The steel rod to be tested is the Japan 7 mm piano steel rod. The load dependence of the magnetic properties of the piano steel rod was manifested. Two experimental designs of U-shape magnetoelastic sensors were introduced, one with double pick-up concentric coils wound on the rod to be tested, the other with pick-up coil on one yoke foot. The former design is used to derive the correlation of the relative permeability with elastic tension, while the latter is aimed to reflect the stress induced magnetic flux variation along the magnetic circuit. Magnetostatic simulations provide interpretations for the yoke foot sensing technology. Tests with double pick-up coils indicate that under proper working points (primary voltages), the relative permeability varies linearly with the axial load for the Japan 7 mm piano steel rod. Tests with pick-up coil on the yoke foot show that the integrated sensing voltage changes quadratically with the load, and error is more acceptable when the working point is high enough.

**Key words:** magnetoelastic sensors; concentric coils; magnetoelastic simulation; permeability; magnetic flux.

## 1. Introduction

It has long been known that the magnetic properties of the ferromagnetic material vary with stress (Joule 1842, Bozorth 1951, Mix 1987, Stablik and Jiles 1993). Such observation has been used in the Non Destructive Examination of the steel structures. Magnetoelastic characterization remains to be one of the most effective technologies in non-destructive examination of steel tendons and cables (Wang, Koontz and Jarosevic 1998, Chen 1999, Singh, Lloyd and Wang 2003). Currently, the predominant magnetic technology in non-contact stress sensing of infrastructure is the solenoid system, in which two coils are wound on the steel sample – primary coil and sensing coil. The primary coil provides variable magnetic flux to the sample while the sensing coil picks up the induced electromotive force that is directly proportional to the change rate of the applied magnetic flux. With pulsed primary current fixed, the relative permeability of the steel rod can be derived from

$$\mu_r(\sigma, T) = 1 + \frac{A_0}{A_f}\left[\frac{V_{out}(\sigma, T)}{V_0} - 1\right] \tag{1}$$

---

† Ph.D. Candidate
‡ Professor

where $\mu_r$ means relative permeability, $\sigma$ is stress, $T$ stands for temperature, $A_0$ and $A_f$ represent cross areas of the sensing coil and the steel rod, respectively. $V_{out}$ is the integrated output (sensing) voltage when the steel rod is under tension $\sigma$, and $V_0$ is the integrated output voltage without ferromagnetic material present in the sensing coil (Wang, Chen, Koontz and Lloyd 2000).

Another approach to deriving the relative permeability is through double pick-up coils (Kvasnica and Fabo 1996), which does not require the measurement of $V_0$, as in Eq. (1). In this approach, it is assumed that the magnetic field is homogeneous within the outside pick-up coil C2, through which the magnetic flux variation within a short time can be expressed as

$$\Delta\Phi_2 = N[A_f\,\Delta B + (A_{02} - A_f)\mu_0\Delta H], \tag{2}$$

in which $N$ is the number of turns of the outside pick-up coil, $A_f$ and $A_{02}$ are the cross area of the rod and the outside pick-up coil respectively, $\Delta H$ is the magnetic field density variation within the coil, $\Delta B$ means the magnetic induction variation along the steel rod, and $\mu_0$ is the permeability of the air. Similarly, through the inner pick-up coil C1, the magnetic flux variation is

$$\Delta\Phi_1 = N[A_f(\Delta B) + (A_{01} - A_f)\mu_0(\Delta H)], \tag{3}$$

where $N$ is the number of turns of the inner pick-up coil, $A_{01}$ is the cross area of the inner pick-up coil. Note that there are $N$ turns for each pick-up coil.

Subtracting (3) from (2) yields

$$\Delta\Phi_2 - \Delta\Phi_1 = N(A_{02} - A_{01})\,\mu_0(\Delta H). \tag{4}$$

Dividing (3) by (4), we have

$$\frac{\Delta\Phi_1}{\Delta\Phi_2 - \Delta\Phi_1} = \frac{A_f}{A_{02} - A_{01}}\mu_r + \frac{A_{01} - A_f}{A_{02} - A_{01}}, \tag{5}$$

in which $\mu_r$ is the relative permeability of the steel rod, $\mu_r = \dfrac{\Delta B}{\mu_0\Delta H}$.

The voltages introduced in the two concentric pick-up coils can be integrated using two electric integrators. The output voltage from the outside pick-up coil is

$$V_{out2} = -\frac{1}{RC}\int_{t_1}^{t_2}\left(-\frac{d\Phi_2}{dt}\right)dt = \frac{1}{RC}(\Phi_2(t_2) - \Phi_2(t_1)) = \frac{\Delta\Phi_2}{RC}, \tag{6}$$

where $t_2$ and $t_1$ are time boundaries of the pulsed pick-up voltage range (reflecting primary current range), and RC is a time constant. In the same way, for the inner pick-up coil:

$$V_{out1} = \frac{\Delta\Phi_1}{RC}. \tag{7}$$

From (5), (6) and (7) there is

$$\frac{V_{out1}}{V_{out2} - V_{out1}} = \frac{\Delta\Phi_1}{\Delta\Phi_2 - \Delta\Phi_1} = \frac{A_f}{A_{02} - A_{01}}\mu_r + \frac{A_{01} - A_f}{A_{02} - A_{01}}, \tag{8}$$

Therefore the relative permeability $\mu_r$ can be calculated from the integrated sensing voltages.

In this research, for the convenience of operation, the primary coil on U-shape yoke is substituted for the solenoid primary coil. Two designs are described separately, one (I) is based on Eq. (8) and the other (II) is based on the magnetic circuit theory.

  I. Double pick-up coils are employed in the measurement of the permeability of the steel rod, with primary coil wound on the U-shape yoke. This trial of remote primary coil has been undertaken in the Univ. of Ill. at Chicago (Wang, Lloyd and Hovorka 2001). The design resembles permeameter (Cullity 1972). This strategy is a celebrated improvement compared to the solenoid approach where hundreds or thousands of primary coil turns are needed to wind on the steel rod to be tested.

 II. Another objective in this research is to design an EM sensor that is detachable from the steel rod. In this research, both primary and sensing coils are designed to be removable. It is known that the flux density along the magnetic circuit depends on the magnetic resistance (Popovic and Popovic 1999). In the magnetic circuit composed of ferrite yoke and steel rod, if the magnetic resistance of the steel changes due to the stress variation, the flux across the yoke section changes as a response. An EM tension sensor based on this phenomenon is designed in the Infrastructures Sensor Technology Laboratory of the Univ. of Ill. at Chicago. This design is more convenient in application than the previous one, because both primary and secondary coils are detachable. However, the detachable EM sensor indirectly senses the stress dependence of the magnetic properties of the steel, and requires a strict consistence of ferromagnetic surroundings in calibration.

In this research, the load sensing technologies using yoke - double pick-up coils system and yoke - coil on the yoke foot system are demonstrated through tests and magnetostatic simulation.

## 2. Experiments

The measurement of hysteresis curves and anhysteresis curves under various stresses is conducted through several computed controlled blocks shown in Fig. 1. Primary solenoid coil or coil with silicon steel yoke can be employed in the magnetization of the ferromagnetic material (steel rod in this research) to be tested. Current running through the primary coil is supplied by the current source. Integrated sensing voltage from the secondary (pick-up) coils reflects the magnetic flux variation along the material to be tested. The tangential magnetic field in the material is extrapolated through three hall sensors with different radical distances from the steel rod (Havorka 2002).

The primary coil is wound on the yoke, pick-up coils are either wound on the specimen, as shown in Fig. 2, or on the yoke foot, as shown in Fig. 3. It was made sure that there was no air gap between the steel rod and the yoke feet. The yoke was stacked from grain-oriented silicon steel laminations, which has a lower magnetic coercive force compared to average steels. The specimen to be tested is galvanized Piano steel rod made in Japan with a diameter of 7 mm. The thickness of the Zinc coating is around 65 $\mu$m. The yield strength and tensile strength are 201,400 psi (1.390 Mpa) and 240,900 psi (1,661 Mpa) respectively. Axial stress without exceeding the yield strength is added stochastically through the hydraulic loading system. Computer software controls the supplication of pulsed primary currents and the acquisition of the pick-up voltages. The magnetostatic simulation results are shown for the technological interpretation.
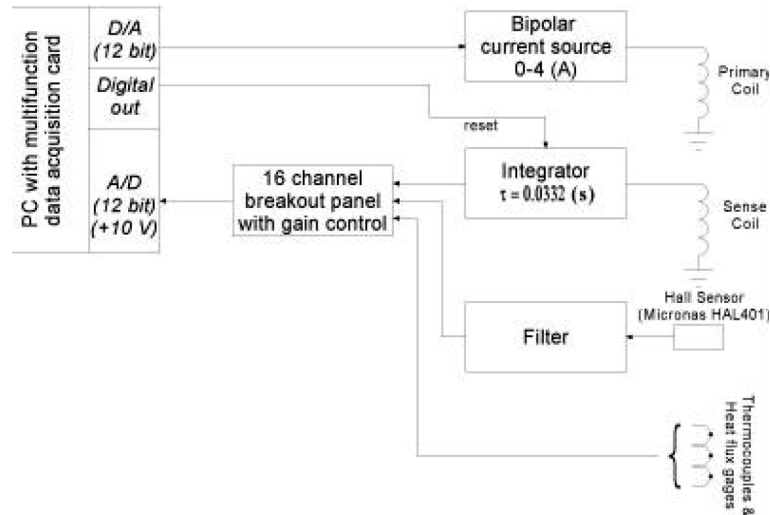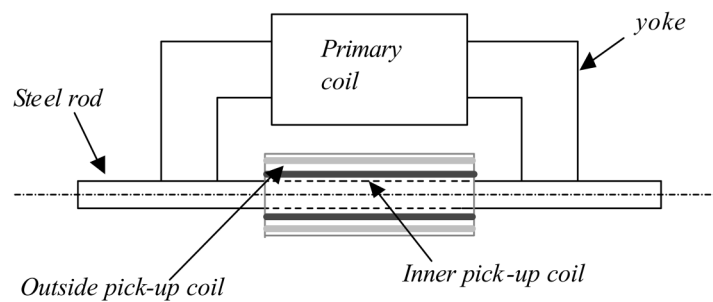
Fig. 1 Block diagram of the magnetic measuring system



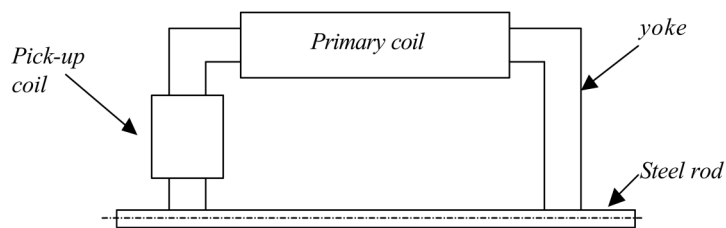Fig. 2 Schematic sketch of EM sensor with double pick-up coils



Fig. 3 Schematic sketch of EM sensor with pick-up coil on one yoke

## 3. Results and analysis - double concentric pick-up coils

Theory and tests indicated that stress affects the magnetic properties of the magnetostrictive materials (Hovorka 2002). Fig. 4 and Fig. 5 show the axial tension dependence of hysterisis and anhysterisis curves of the Japan 7 mm piano steel rod, respectively.
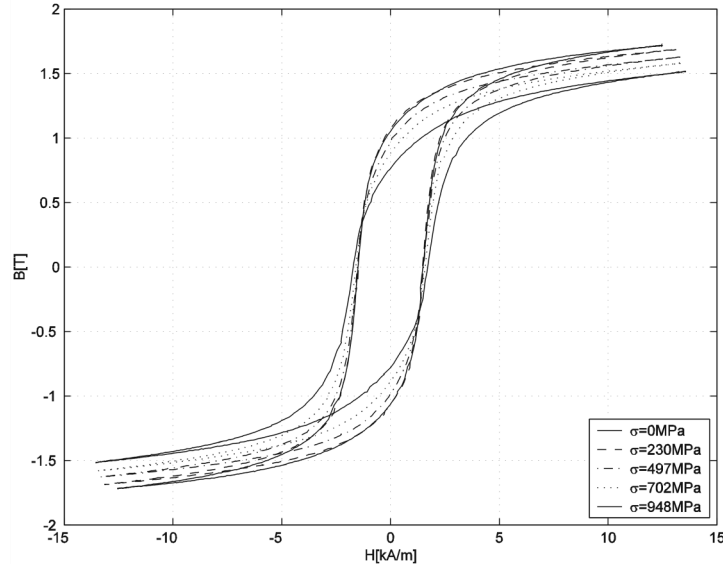
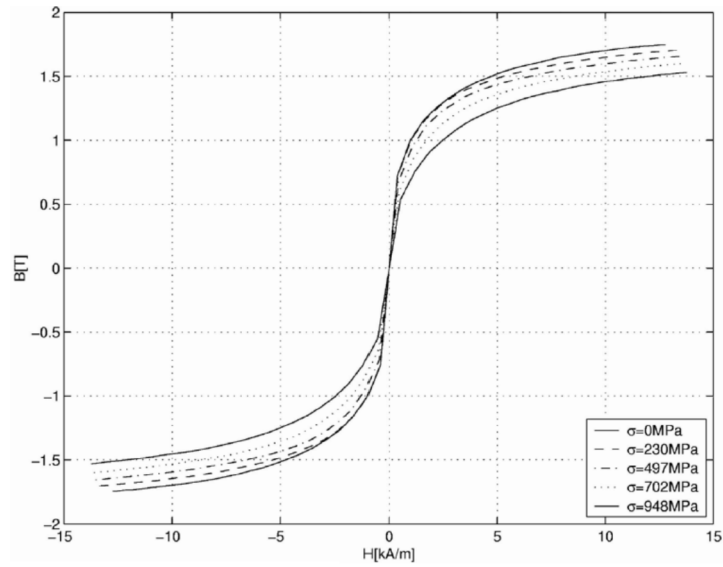Fig. 4 Hysteresis curves of the Japan 7 mm piano steel rod at different applied tensile stresses



Fig. 5 Anhysteresis curves of the Japan 7 mm piano steel rod at different applied tensile stresses

Although not completely detachable, the yoke-double sensing coils system does not require winding primary coil on the steel rod. At a given working point (primary voltage value, proportional to primary current) and axial tensile load, the permeability of the steel rod is calculated through Eq. (8). Fig. 6 shows the correlation of load and permeability, when the double concentric pick-up coils are placed in the middle of the yoke. It indicates that the higher the working point is, the more linear the load-permeability correlation becomes. If the double pick-up coils together move close

enough to the yoke foot, the relative permeability changes more linearly with load, as indicated in Fig. 7. This is because the steel rod can be magnetically saturated more easily at the location close to the yoke foot, which was proven in the magnetic simulation shown in Fig. 8 (for reference, the saturated induction of the Japan piano rod is around 2T.). The B field distribution along the rod and the yoke is shown in Fig. 9. The result in Fig. 7 is consistent with the observation that there is a highly linear correlation between relative permeability and tension, only when the steel is nearly magnetic saturated (Wang, Chen, Koontz and Lloyd 2000). Without the sensor relocated, the error is below 3% and repeatability is good. Indeed the data for each curve was composed of results from several cycles of test, with deviation no larger than 1%. The simulation results in Fig. 8 indicate that saturated magnetization can be achieved even in the middle of the rod between the yoke feet, provided that the current density is high enough. Although it is much easier to derive a linear correlation between calculated relative permeability and load when the double pick-up coils are
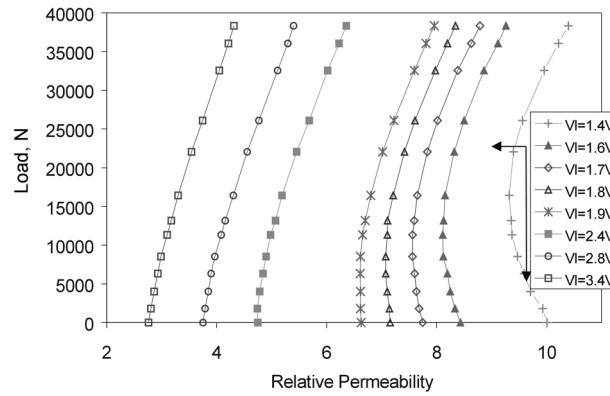


Fig. 6 Test result of load sensing using U-shape EM sensor with double concentric pick-up coils in the middle of the yoke, integration range of the primary voltage: $V_{high} - V_{low}$(VI in the graph) = 0.1 V (elastic load limit of the Japan 7 mm piano rod: 53.5 KN)
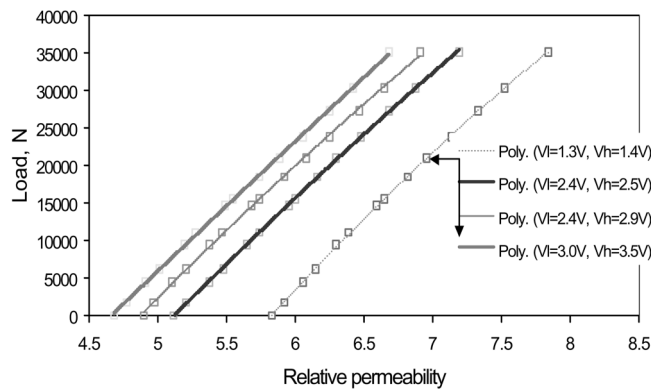


Fig. 7 Test results of load sensing using U-shape EM sensor with double pick-up coils close to the yoke foot, Vh and Vl being the high and low integration boundaries of the primary voltage (elastic load limit of the Japan 7 mm piano rod: 53.5 KN)
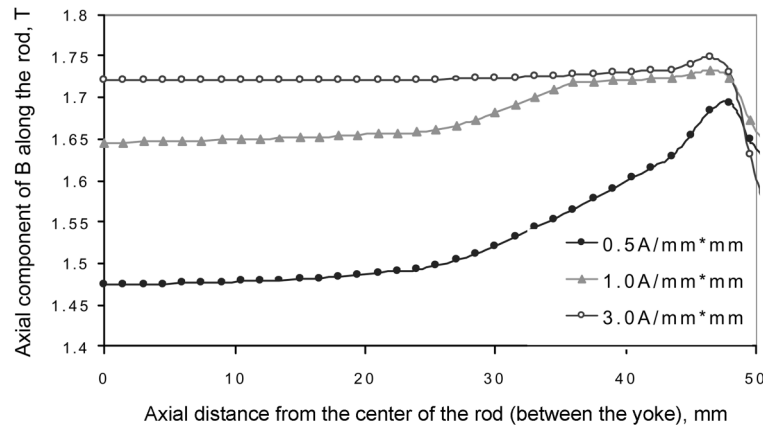
Fig. 8 Magnetostatic simulation result: Magnetic field density along the steel rod, legend indicating the current density in the primary coil, the distance between the yoke being 103 mm
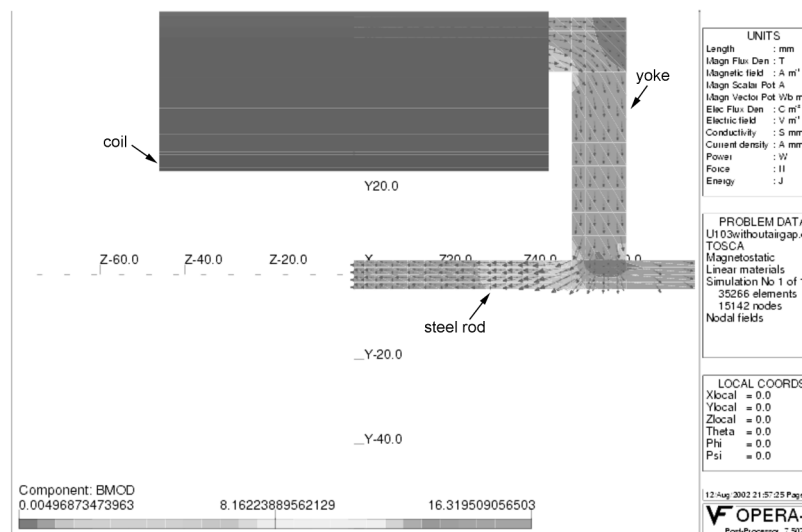


Fig. 9 Magnetostatic simulation result: B field distribution in the rod and the yoke

placed closely to the yoke foot, the interpretation for the permeability measured is different from that with the sensing coils in the center. Along the axial direction of the rod, as distance from the center increases, the radial component of B field increases as well. However, the sensing coils only pick up the variation of the B field's *axial* component field. Besides, the B field's *axial* component near the yoke foot is not so homogeneous as its counterpart in the center, as observed from the simulation results shown in Fig. 8. Therefore, the permeability derived from the sensing coils close to the yoke foot is not strictly in accordance with the definition of relative permeability.

## 4. Results and analysis - pick-up coil on the yoke foot

U-shape sensors with pick-up coils on the yoke foot are not designed to directly measure the magnetic flux variation through the coil wound on the rod, but rather indirectly through the coil wound on the yoke foot. The sketch is shown in Fig. 3.

For an ideal closed magnetic circuit,

$$\sum NI - \sum R_m \phi_m = 0, \tag{9}$$

Where $N$ is the number of turns of the primary coil, and $I$ is the primary current, $R_m = \int_C \dfrac{dl}{\mu A}$, which

is called the magnetic resistance of each section of the magnetic circuit, where $l$ is the length of the integration route C, $\mu$ is the permeability of each material, and A is the cross area (Popovic and Popovic 1999).

Theoretically, at any node of the magnetic circuit,

$$\sum \Phi = 0. \tag{10}$$

In the circuit composed of an U-shape sensor and steel rod, if the permeability of the steel rod changes, the magnetic resistance of the steel rod changes accordingly, which leads to magnetic flux variations along the circuit. Under the ideal condition, the absolute flux variation at any node along the circuit should be the same. However, in the magnetic circuit of ferrite yoke and steel rod, due to the magnetic leakage through the air and the steel rod beyond the circuit, the absolute magnetic flux varies from node to node. As a result, the flux along the rod is less than that along the yoke foot, as given in the following equation:

$$\phi_{yoke} = p\,\phi_{rod} \tag{11}$$

where $\phi_{yoke}$ and $\phi_{rod}$ are respectively the flux along the yoke foot and the rod, $p$ is a function of magnetic parameters of the rod and yoke, and the primary voltages, as well as the geometric characters of the magnetic circuit. Eq. (11) can be demonstrated through magnetostatic simulation. First, the B field distribution along the steel rod and yoke foot is demonstrated, then the value of function $p$ in Eq. (11) is calculated for various primary voltages. The simulation results of flux density along the steel rod and yoke foot under various primary current densities are given in Fig. 8 and Fig. 10. Fig. 11 shows how $1/p$ ($p = \phi_{yoke}/\phi_{rod}$) varies with current density, which also indicates that the $p$ value tends to be constant as current density increases.

For a certain yoke (steel rod magnetic circuit as shown in Fig. 3), we also have

$$\phi_{rod} = f(V_{Primary}, F, A_{rod}), \tag{12}$$

where $V_{Primary}$, $F$, $A_{rod}$, axial load, and cross area of the rod, respectively. However, $\phi_{rod}$ is also related to some other factors such as the permeability of the rod, although those factors of main concern here. From Eqs. (11) and (12)

$$\phi_{yoke} = p \bullet f(V_{Primary}, F, A_{rod}) = g(V_{Primary}, F, A_{rod}). \tag{13}$$
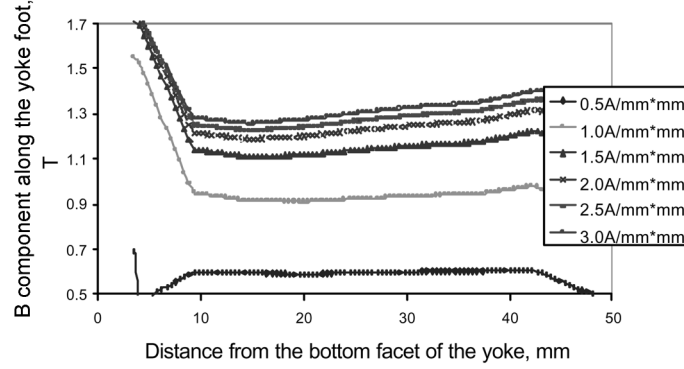
Fig. 10 Magnetostatic simulation result: Magnetic field density along the yoke foot, the legend indicates current density in the primary coil

With pulsed current in the primary coil, the induced integrated pick-up voltage is proportional to the magnetic flux variation. Therefore, Eq. (13) can be rewritten as

$$V_{integrated} = \varphi\,(F,\ V_{pulsed\text{-}Primary},\ A_{rod}). \tag{14}$$

Where $V_{integrated}$ is the integrated voltage from the pick-up coil wound on the yoke foot, and $V_{pulsed\text{-}Primary}$ is the pulsed primary voltage indicating the primary current according to Ohm's Law.

Through test, the correlation of load $F$ and integrated pick-up voltage, $V_{integrated}$, is demonstrated in Fig. 11. It should be noted that to reduce the adverse effect of magnetic remanence in the rod, the transient primary current should be high enough to saturate the steel rod. Fig. 12 shows that tension varies quadratically with the integrated pick-up voltage. Tests also indicate some parallel shifts in the curves from test to test, as Fig. 13 indicates. These shifts may be caused by the various leakage of the flux in the ferrite yoke-steel rod circuit and the magnetic remanence. However, under certain pulsed primary current, if the initial (without load) integrated voltages are calibrated to the same value, the correlation of load and integrated voltage is almost fixed, as demonstrated in Fig. 14.
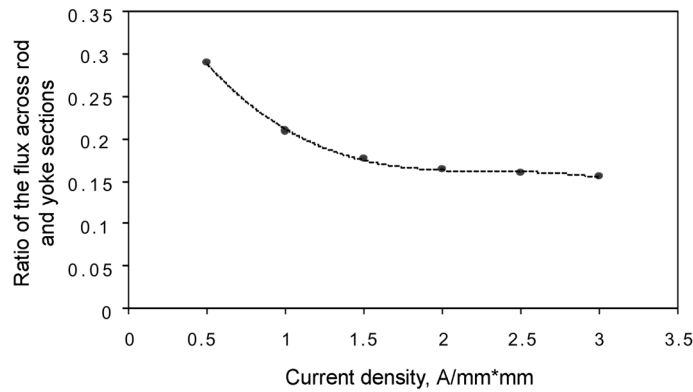


Fig. 11 Magnetostatic simulation result: Ratio of the magnetic flux across the rod and yoke foot section as a function of current density (with the calculation of the magnetic flux across the cross section of the rod and yoke foot in their longitudinal middle positions)
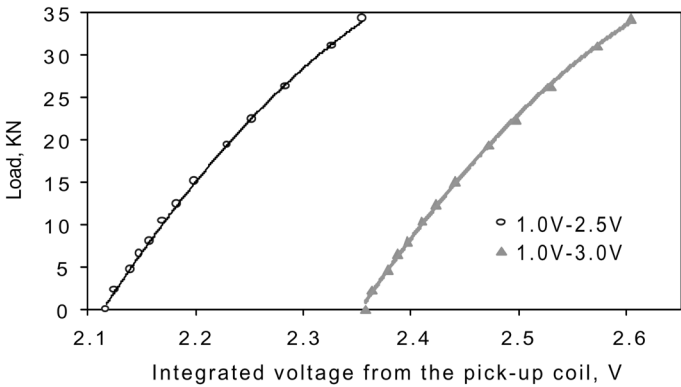
Fig. 12 Test results of EM sensor with pick-up coil on the yoke foot, legend indicating the working point (elastic load limit of the Japan 7 mm piano rod: 53.5 KN)
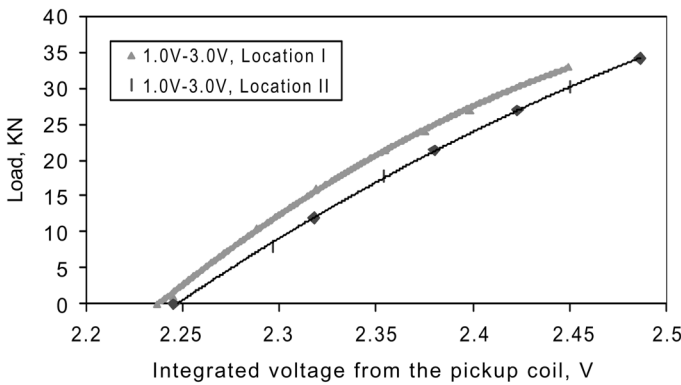


Fig. 13 Load measurement in Japan 7 mm rod using U-shape EM sensor with pickup coil wound on the yoke, legend indicating the working point
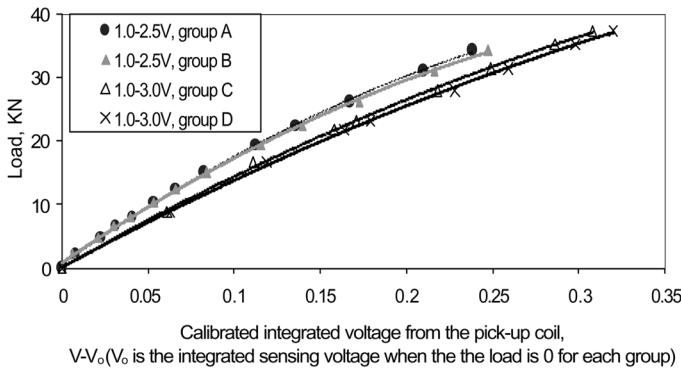


Fig. 14 Correlation of load versus calibrated integrated pick-up voltage (elastic load limit of the Japan 7 mm piano rod: 53.5 KN)
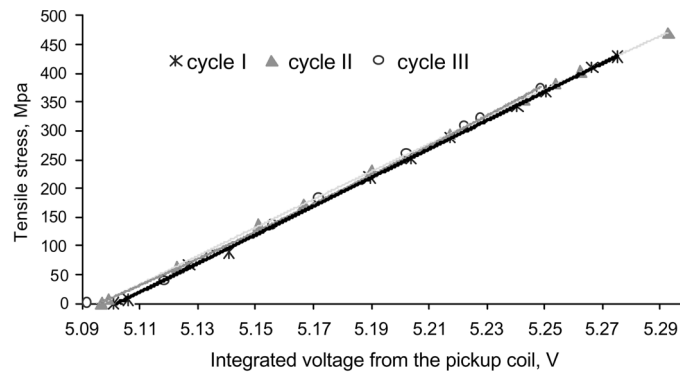
Fig. 15 Stress monitoring of the 0.5 inch steel strand using U shape EM sensor, working point 4.0-7.0 V

Table 1 Magnetostatic simulation result: Value of $\Phi_{rod}/\Phi_{yoke}$ versus yoke gap, $\Phi_{rod}$ and $\Phi_{yoke}$ being respectively the magnetic flux across the cross section of steel rod and yoke foot in the middle of their length (in $(\Phi D - \Phi d) \times h$, $D$ is the outside diameter, $d$ is the inner diameter of the primary coil, and $h$ is the length of the coil)

| Yoke gap, mm | coil dimension, mm | $B_{rod}$, T | $B_{yoke}$, T | $\Phi_{rod}/\Phi_{yoke}$ |
|---|---|---|---|---|
| 103 | $(\Phi30 - \Phi14) \times 90$ | 1.65 | 0.92 | 20.9% |
| 90 | $(\Phi30 - \Phi14) \times 84$ | 1.67 | 0.88 | 22.1% |
| 80 | $(\Phi30 - \Phi14) \times 74$ | 1.68 | 0.84 | 23.3% |
| 70 | $(\Phi30 - \Phi14) \times 64$ | 1.68 | 0.78 | 25.1% |
| 60 | $(\Phi30 - \Phi14) \times 54$ | 1.65 | 0.64 | 30.1% |

It can be observed that a good calibration gives an error below $\pm 5\%$. Fig. 14 indicates that the higher the working point, the better the resolution becomes. Tests also show that a load variation of 200 N (5.2 Mpa) can be detected. Fig. 15 indicates that U shape EM sensor gives satisfactory repeatability, especially at higher loads, provided that the location of the U shape EM sensor remains the same. Table 1 shows that with yoke gap (the distance between the yoke feet) reduced, it is more efficient for the induction to be transferred from the yoke to the steel rod. In order to minimize the influence of magnetic remanence, we can either increase the turns of the primary coil or the current density. The demagnetizing process is advised as well.

## 5. Conclusions

Two U-shape EM sensor designs for load sensing have been demonstrated. In the yoke - double concentric pick-up coils system, the double concentric coils should be placed as closely as possible to the yoke foot. Between permeability and tensile load, a nearly linear correlation was observed. Regarding the design with pick-up coils on the yoke foot, integrated pick-up voltage varies quadratically with load, while the drawback of parallel shift of load - integrated sensing voltage curve should be minimized by modifications in design and operation. It is noted that temperature influence should be studied extensively in the field utility of EM sensor with remote coil. The heat

flux and the temperature gradient in the solenoid coil system, as well as their effects on the magnetic property of the Japan piano steel were systematically studied by Lloyd *et al.* (Lloyd, Singh and Wang 2002). Temperature as a factor in the remote coil system is more complicated because it involves not only the steel rod to be tested, but the ferrite yoke to be tested as well.

## References

Bozorth, R.M. (1951), *Ferromagnetism*, D. Van Nostrand Company, INC., Canada.

Chen, Z.L. (1999), "Characterization and constitutive modeling of ferromagnetic materials for measurement of stress", PhD thesis, the Univ. of Ill. at Chicago.

Cullity, B.D. (1972), *Introduction to Magnetic Materials*, Addision-Welsley, Publishing Company, Reading MA.

Daughton, J.M. (1999), "GMR applications", *J. Magn. Magn. Mat.*, **192**, 334-342.

Hovorka, O. (2002), "Measurement of hysteresis curves for computational simulation of magnetoelastic stress sensors", MS thesis, the Univ. of Ill. at Chicago.

Joule, J.P. (1842), "On a new class of magnetic forces", *Ann. Electr. Magn. Chem.*, **8**, 219-224.

Kvasnica, B. and Fabo, P. (1996), "Highly precise non-contact instrumentation for magnetic measurement of mechanical stress in low-carbon steel wires", *Meas. Sci. Tech.*, 763-767.

Lloyd, G.M., Singh, V. and Wang, M.L. (2002), "Experimental evaluation of differential thermal errors in magnetostatic stress sensors for Re < 180", IEEE Sensors 2002, Magnetic Sensing III, Paper No. 6.54.

Mix, P.E. (1987), *Introduction to Nondestructive Testing*, John Wiley & Sons, Inc., Hoboken, NJ.

Popovic, Z. and Popovic, B.D. (1999), *Introductory Electronics*, Prentice Hall, Inc., Upper Saddle River, NJ.

Singh, V., Lloyd, G.M. and Wang, M.L., "Effects of temperature and corrosion thickness and composition on magnetic measurements of structure steel wires", the 6th ASME-JSME 2003, accepted.

Stablik, M.J. and Jiles, D. (1993), "Coupled magnetoelastic theory magnetic and magnetostrictive hysteresis", *IEEE Trans. Magn.*, **29**, 2113-2123.

Wang, M.L., Chen, Z.L., Koontz, S.S. and Lloyd, G.D. (2000), "Magneto-elastic permeability measurement for stress monitoring", In *Proceeding of the SPIE 7th Annual Symposium on Smart Structures and Materials*, Health Monitoring of the Highway Transportation Infrastructure, 6-9 March, CA, **3995**, 492-500.

Wang, M.L., Koontz, S. and Jarosevic, A. (1998), "Monitoring of cable forces using magneto-elastic sensors", *2nd U.S.-China Symposium workshop on Recent Developments and Future Trends of Computational Mechanics in Structural Engineering*, May 25-28, Dalian, PRC. 337-349.

Wang, M.L., Lloyd, G. and Hovorka, O. (2001), "Development of a remote coil magneto-elastic stress sensor for steel cables", *SPIE 8th Annual International Symposium on Smart Structures and Material*, Health Monitoring and Management of Civil Infrastructure Systems; Newport Beach CA, **4337**, 122-128.